

## Anomalous metallic ground state in $\text{BaV}_{13}\text{O}_{18}$

T. Kanzaki,<sup>1</sup> J. Fujioka,<sup>2</sup> Y. Tokura,<sup>2</sup> H. Kuwahara,<sup>3</sup> and T. Katsufuji<sup>1,4,\*</sup>

<sup>1</sup>*Department of Physics, Waseda University, Tokyo 169-8555, Japan*

<sup>2</sup>*Department of Applied Physics, University of Tokyo, Tokyo 113-8656, Japan*

<sup>3</sup>*Department of Physics, Sophia University, Tokyo 169-8555, Japan*

<sup>4</sup>*Kagami Memorial Laboratory for Material Science and Technology, Waseda University, Tokyo 169-0051, Japan*

(Received 21 January 2014; revised manuscript received 19 March 2014; published 1 April 2014)

We studied single crystals of  $\text{BaV}_{13}\text{O}_{18}$ , in which V ions with an average valence of  $+2.62$  ( $3d^{2.38}$ ) form a quasi-fcc lattice. We found that the ground state of the stoichiometric crystal is insulating, whereas that of the off-stoichiometric crystal is metallic with a large effective mass. This metallic state can be explained by the Kondo coupling between the magnetic moment existing at the lone V ion and itinerant carriers in the V tetramers.

DOI: [10.1103/PhysRevB.89.140401](https://doi.org/10.1103/PhysRevB.89.140401)

PACS number(s): 75.20.Hr, 75.25.Dk, 78.30.-j

Recently, it has been reported that hexagonal  $\text{AV}_{13}\text{O}_{18}$  ( $A = \text{Ba, Sr}$ ), in which the average valence of V ions is  $+2.62$  (the average number of  $d$  electrons per V is 2.38), exhibits a variety of phases [1,2]. In this series of compounds, V and O ions occupy a part of the NaCl structure, and thus, V ions form a quasi-fcc lattice with periodically missing sites [3,4]. The high-temperature phase of this series of compounds is characterized by a lone V ion at the center, surrounded by six V tetramers, each of which has a rhombus shape composed of two regular triangles connected at the edge, as illustrated in the upper panel in Fig. 1. Experimentally, these tetramers start to form below  $\sim 800$  K, and the magnetic susceptibility keeps decreasing with decreasing temperature ( $T$ ) below 800 K, indicating a spin-singlet formation. This V tetramerization is likely caused by an orbital ordering of V  $t_{2g}$  states. The absence of a structural phase transition associated with this orbital ordering can be attributed to the fact that the orbital ordering and the resultant formation of V tetramers do not break the symmetry of the original crystal structure [2].

Among this series of compounds,  $\text{SrV}_{13}\text{O}_{18}$  exhibits a structural phase transition at  $T_{\text{tr}} = 270$  K [1]. Below  $T_{\text{tr}}$ , the lone V ion at the center forms a V trimer with two V ions of the surrounding two tetramers, and the two tetramers are accordingly changed into two trimers; thus 13 V ions are separated into three trimers and one remaining tetramer. Note that such a trimerization of V ions at low  $T$  was observed in various vanadates in which  $\text{V}^{3+}$  ( $3d^2$ ) ions form a quasi-fcc lattice [5,6] and was attributed to the orbital ordering of V  $t_{2g}$  states [7]. The resistivity and magnetic susceptibility of  $\text{SrV}_{13}\text{O}_{18}$  decrease at  $T_{\text{tr}}$ . On the other hand,  $\text{BaV}_{13}\text{O}_{18}$  exhibits a different type of phase transition at  $T_{\text{co}} \sim 200$  K [1]. There is no discernible change in the powder x-ray diffraction, unlike the case of  $\text{SrV}_{13}\text{O}_{18}$  at  $T_{\text{tr}}$ , but superlattice peaks at  $(0, 1/2, 1/2)$  appear in the electron diffraction below  $T_{\text{co}}$ . This suggests that there is no substantial change in the configuration of V tetramers and lone V ions, but a charge ordering occurs for the lone V ion in  $\text{BaV}_{13}\text{O}_{18}$ .

Characteristics of the ground state in  $\text{BaV}_{13}\text{O}_{18}$  are not clear. The resistivity of polycrystalline  $\text{BaV}_{13}\text{O}_{18}$  increases at  $T_{\text{co}}$  and keeps increasing with further decreases in  $T$ , but the absolute value of the resistivity at the lowest  $T$

remains  $\sim 1 \Omega \text{ cm}$  [1], which is much lower than that of other Ba-V-O compounds exhibiting an insulating ground state with V trimerization ( $\text{BaV}_{10}\text{O}_{15}$  [5] and  $\text{Ba}_2\text{V}_{13}\text{O}_{22}$  [6]). The magnetic susceptibility of  $\text{BaV}_{13}\text{O}_{18}$  exhibits a small drop at  $T_{\text{co}}$  but increases with further decreases in  $T$ , indicating a Curie-Weiss behavior, whose Curie constant is consistent in size with magnetic moments ( $S = \frac{1}{2}-1$ ) existing only on lone V ions. According to the phase diagram of  $\text{Ba}_{1-x}\text{Sr}_x\text{V}_{13}\text{O}_{18}$  in polycrystalline forms, the transition temperature  $T_{\text{tr}}$ , which is 270 K for  $\text{SrV}_{13}\text{O}_{18}$  ( $x = 1$ ), decreases with decreasing  $x$  (increasing the Ba content) but survives even in  $\text{BaV}_{13}\text{O}_{18}$  at  $\sim 70$  K [2]; thus, there are two phase transitions in  $\text{BaV}_{13}\text{O}_{18}$ . However, anomalies in the resistivity and magnetic susceptibility are barely observed at  $T_{\text{tr}} \sim 70$  K in polycrystalline  $\text{BaV}_{13}\text{O}_{18}$ , in clear contrast to the anomalies observed at  $T_{\text{co}} \sim 200$  K.

It is known that such an orbital/charge ordering is fragile against disorder and that the transport properties of polycrystalline samples are seriously affected by the grain boundaries. In this paper, we report the physical properties of  $\text{BaV}_{13}\text{O}_{18}$  single crystals. We studied two single crystals, both of which exhibit a high- $T$  phase transition ( $T_{\text{co}}$ ), but only one of which exhibits a low- $T$  phase transition, at  $T_{\text{tr}} = 65$ . We found that the ground state of the sample exhibiting  $T_{\text{tr}}$  is insulating, whereas the sample without  $T_{\text{tr}}$  exhibits a metallic ground state with a large effective mass. This mass enhancement can be explained by the Kondo coupling between localized magnetic moments at the lone V ions and itinerant carriers in V tetramers.

Single crystals of  $\text{BaV}_{13}\text{O}_{18}$  were grown by the floating-zone technique. Details of the crystal growth and characterization are given in the Supplemental Material [8]. Electrical resistivity was measured by a conventional four-probe method. Magnetic susceptibility was measured by a SQUID magnetometer. Specific heat was measured by a relaxation method. Optical reflectivity was measured between 0.01 and 0.8 eV by FTIR spectrometers and between 0.7 and 5 eV by a grating spectrometer. In the following, we discuss two single crystals of  $\text{BaV}_{13}\text{O}_{18}$  (samples 1 and 2). Thermogravimetric analysis indicates that with the notation of  $\text{BaV}_{13}\text{O}_{18+\delta}$ ,  $\delta$  is 0.1 for sample 1 and 0.8 for sample 2; sample 1 is close to stoichiometric.

Figures 1(a) and 1(b) show the  $T$  dependence of resistivity for the two single crystals with  $j \parallel a$  ( $\rho_a$ ) and  $j \parallel c$  ( $\rho_c$ ). As can be seen,  $\rho_c$  is smaller than  $\rho_a$  over the whole  $T$  range for

\*katsuf@waseda.jp

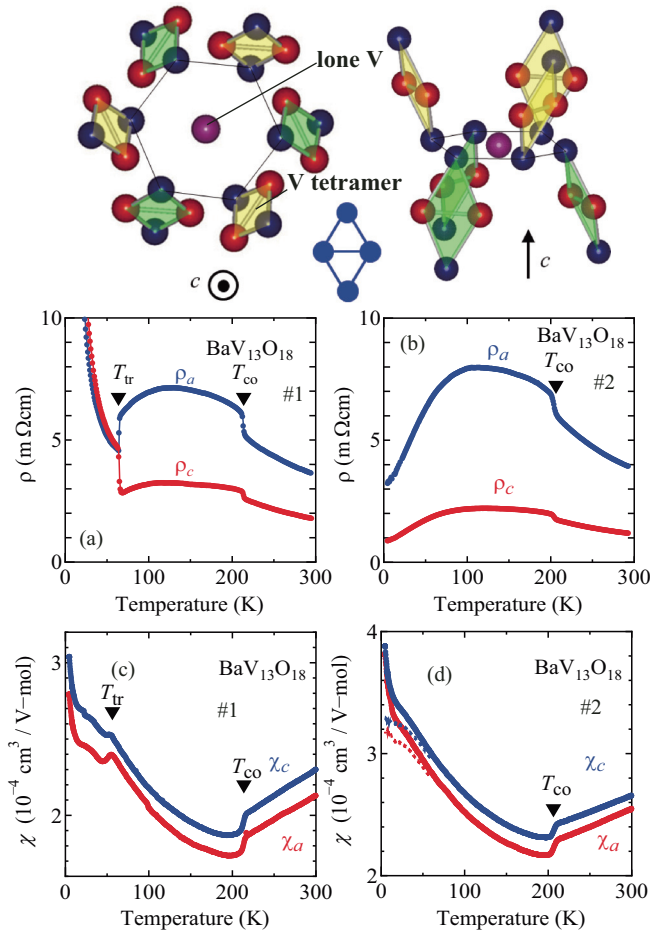


FIG. 1. (Color online) Top: Arrangement of V ions in  $\text{BaV}_{13}\text{O}_{18}$ : the lone V ion at the center and six surrounding V tetramers. The left panel is a top view and the right is a side view. (a, b) Temperature dependence of resistivity for (a) sample 1 and (b) sample 2 of  $\text{BaV}_{13}\text{O}_{18}$ . (c, d) Temperature dependence of magnetic susceptibility for (c) sample 1 and (d) sample 2. Dashed lines correspond to the susceptibility from which the low- $T$  Curie component is subtracted.

sample 2 and above 65 K for sample 1. This is likely related to the facts that the electron transfer along the V tetramer is dominant over that between tetramers or between a lone V and a tetramer and that the longer diagonal axis of the tetramer is tilted by only  $\sim 19^\circ$  from the  $c$  axis (upper right panel in Fig. 1); thus the electrons can travel more easily along the  $c$  axis. For both samples (nos. 1 and 2), there is an anomaly of resistivity at  $T_{\text{co}} \sim 200$  K, where both  $\rho_a$  and  $\rho_c$  increase with decreasing  $T$ . Another anomaly at  $T_{\text{tr}} = 65$  K exists only in sample 1, where  $\rho_c$  increases while  $\rho_a$  decreases with decreasing  $T$ , but both  $\rho_a$  and  $\rho_c$  increase with further decreases in  $T$ . On the other hand, both  $\rho_a$  and  $\rho_c$  for sample 2 decrease with decreasing  $T$  below  $\sim 100$  K down to the lowest  $T$ , indicating a metallic ground state for this sample. We found that the  $T$  dependence of  $\rho$  below 30 K for sample 2 is given by  $\rho = \rho_0 + AT^{1.5}$  for both  $\rho_a$  and  $\rho_c$  [8].

Magnetic susceptibilities of the two samples are shown in Figs. 1(c) and 1(d). The anisotropy of the magnetic susceptibility for  $H \parallel a$  ( $\chi_a$ ) and  $H \parallel c$  ( $\chi_c$ ) is less than 10%, and the behaviors of  $\chi_a$  and  $\chi_c$  are similar to those of the

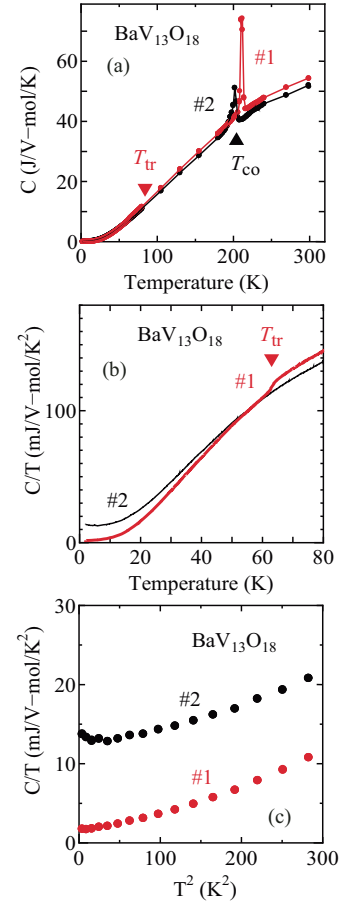


FIG. 2. (Color online) (a) Specific heat ( $C$ ) vs  $T$  below 300 K, (b)  $C/T$  vs  $T$  below 80 K, and (c)  $C/T$  vs  $T^2$  below 55 K for the two crystals (samples 1 and 2) of  $\text{BaV}_{13}\text{O}_{18}$ .

polycrystalline samples [1,2]. For sample 1, there is a small drop in  $\chi$  at  $T_{\text{tr}} = 65$  K.

The result of specific-heat ( $C$ ) measurements is shown in Fig. 2. As shown in Fig. 2(a) ( $C$  vs  $T$ ), there is a large peak in  $C(T)$  at  $T_{\text{co}}$  for both samples. For sample 1, a sharp decrease in  $C(T)$  is observed at  $T_{\text{tr}}$ , which is more clearly shown in Fig. 2(b) ( $C/T$  vs  $T$ ). Note that the present specific-heat measurement was performed by a relaxation method, and thus the release of latent heat by the first-order phase transition at  $T_{\text{tr}}$  may not be fully detected. Figure 2(c) shows  $C/T$  as a function of  $T^2$ . The  $T$  linear coefficient in  $C(T)$ ,  $\gamma$ , arising from the electron specific heat, is  $\sim 12$  mJ/V-mol  $\text{K}^2$  for sample 2 and  $\sim 1$  mJ/V-mol  $\text{K}^2$  for sample 1. The larger value of  $\gamma$  for sample 2 is consistent with the metallic behavior of the same sample regarding the  $T$  dependence of  $\rho$  shown in Figs. 1(b).

It is known that orbital ordering, which is accompanied by V trimerization below  $T_{\text{tr}}$ , is fragile against disorder or carrier doping, and the absence of  $T_{\text{tr}}$  for sample 2 can be attributed to the hole doping induced by excess oxygen.  $\text{BaV}_{13}\text{O}_{18+\delta}$  with  $\delta = 0.8$  means that there are 1.6 holes per 13 V tions, most likely in the three V tetramers. We speculate that these holes in sample 2 are responsible for the suppression of  $T_{\text{tr}}$  and the metallic ground state.

Although the behavior of the specific heat for sample 2 is consistent with its metallic characteristics, the  $T$  dependence

of  $\chi$ , which indicates the existence of the localized moments, does not seem consistent. For this issue, one can see that the behavior of  $\chi(T)$  for sample 2 in Fig. 1(d) below  $\sim 50$  K can be separated into a saturation behavior (as shown by dashed lines) and the remnant Curie behavior. If we assume that the saturation value of  $\chi$ ,  $3.3 \times 10^{-4} \text{ cm}^2/\text{V-mol}$ , arises from a Pauli paramagnetic susceptibility, the Wilson ratio, i.e.,  $\chi/\gamma$  in the unit of  $3\mu_B^2/\pi^2k_B^2$ , is  $\sim 2$ , a typical value for strongly correlated electron systems. This result, together with the Curie-Weiss behavior above 50 K, reminds us of the Kondo behavior. Namely, in higher  $T$  regions ( $> 50$  K), i.e., above the Kondo temperature ( $T_K$ ), there are localized magnetic moments, presumably sitting on the lone V ions, and also itinerant carriers, presumably caused by the holes in the tetramers. In this  $T$  range, the localized moments act as scattering centers for the itinerant carriers, and this causes the negative value of  $d\rho/dT$ . However, at low  $T$  ( $< 50$  K), i.e., below  $T_K$ , the localized moments and itinerant carriers are coupled and form heavy-mass carriers, which are responsible for the metallic conduction at low  $T$ . Assuming that the localized moments exist on lone V ions, and thus, the number of carriers with a heavy mass is only 1/13 the number of total V ions, the electron specific heat  $\gamma = 12 \text{ mJ/V-mol K}^2$  corresponds to an effective mass of  $\sim 50m_0$ , where  $m_0$  is the free electron mass.

We measured the optical reflectivity spectra for no. 1 and 2 crystals polished on the  $ac$  plane and for an as-cleaved no. 2 crystal on the  $(32\bar{2})$  plane. Note that the  $(32\bar{2})$  plane in the present compound corresponds to a  $(100)$  plane of the NaCl structure that the V and O ions form. We found that the spectra for the polished and cleaved surfaces of sample 2 are discernibly different below  $T_{co}$ . This is caused by the remnant stress applied to the sample surface during polishing. Thus, we only show the data taken on the cleaved surface of sample 2 below. Here, the  $(32\bar{2})$  plane contains the axis along the  $ab$  plane ( $[2\bar{3}0]$  axis) but does not contain the  $c$  axis. Thus, we measured the reflectivity on the  $(32\bar{2})$  plane with two polarization directions, along the  $[2\bar{3}0]$  axis ( $R_a$ ) and along the one perpendicular to the  $[2\bar{3}0]$  axis on the  $(32\bar{2})$  plane ( $R_{ac}$ ), as illustrated in the lower-right panel in Fig. 3. The  $R_a$  and  $R_{ac}$  spectra at various temperatures are shown in Figs. 3(a) and 3(b). The optical conductivity spectrum along the  $a$  axis [ $\sigma_a(\omega)$ ] can be directly obtained by Kramers-Kronig transformation of the  $R_a(\omega)$  spectra, whereas that along the  $c$  axis [ $\sigma_c(\omega)$ ] can be calculated by both the  $R_a(\omega)$  and the  $R_{ac}(\omega)$  spectra with a Kramers-Kronig transformation [8].

Figure 3(c) shows the overall features of the  $\sigma(\omega)$  spectra along the  $a$  and  $c$  directions at 300 K. There are three structures in both  $\sigma_a(\omega)$  and  $\sigma_c(\omega)$ : a peak at  $\sim 0.5$  eV, a broad structure between 0.5 and 3 eV, and an edge at  $\sim 4$  eV. These spectral features are similar to those for  $\text{BaV}_{10}\text{O}_{15}$ , shown by the dashed line in Fig. 3(c), in which the V ions form a bilayer slab of a quasi-fcc lattice with periodically missing sites, and the three peaks were assigned to the in-gap excitation (between  $\text{V}^{2+}$  and  $\text{V}^{3+}$ ), Mott excitation (between  $\text{V}^{3+}$  and  $\text{V}^{3+}$ ), and charge-transfer excitation (between  $\text{V}^{3+}$  and  $\text{O}^{2-}$ ), respectively [5,9]. This simple structure of the  $\sigma(\omega)$  spectrum and the similarity between the spectrum of  $\text{BaV}_{13}\text{O}_{18}$  and that of  $\text{BaV}_{10}\text{O}_{15}$  indicate that the electronic structures of these compounds are dominated by a local configuration of the V

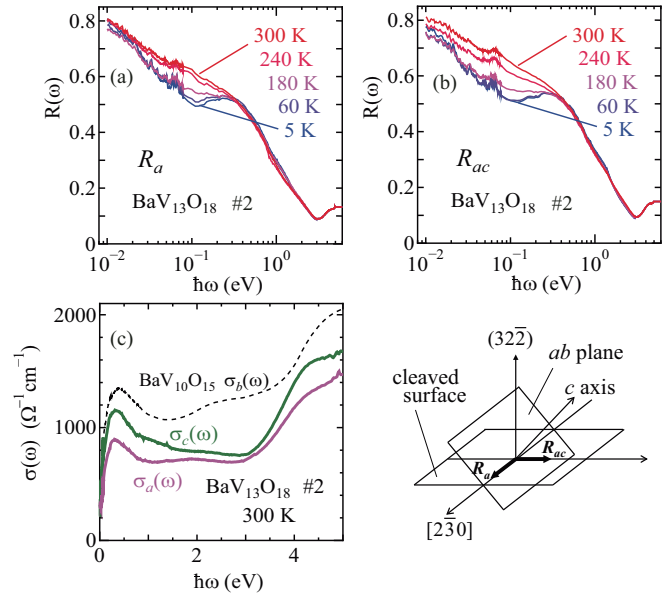


FIG. 3. (Color online) (a, b) Reflectivity spectra at various temperatures on the  $(32\bar{2})$  plane with the polarization directions (a) along the  $[2\bar{3}0]$  axis and (b) perpendicular to the  $[2\bar{3}0]$  axis. (c) Optical conductivity spectra at 300 K derived from the reflectivity spectra, together with that for  $\text{BaV}_{10}\text{O}_{15}$  (along the  $b$  axis). Data for  $\text{BaV}_{10}\text{O}_{15}$  are offset by  $200 \text{ } \Omega^{-1} \text{ cm}^{-1}$  for clarity. Lower right: Configurations of the cleaved surface, crystal axes, and polarization directions for the optical reflectivity measurement.

and O ions with a Coulomb repulsion in the V  $d$  states, rather than the band structure with many branches [10] caused by a large number of ions in a unit cell. Note that the absolute values of  $\sigma_c$  are larger than those of  $\sigma_a$  over the whole  $\hbar\omega$  range ( $0 < \hbar\omega < 5$  eV) for  $\text{BaV}_{13}\text{O}_{18}$ , consistent with the lower values of dc resistivity along the  $c$  axis.

Figures 4(a) and 4(b) show  $\sigma_a(\omega)$  and  $\sigma_c(\omega)$  below 1 eV at various temperatures. Both  $\sigma_a$  and  $\sigma_c$  below 0.25 eV decrease with decreasing  $T$ . However, the conductivity does not become 0 but maintains a finite value ( $\sim 200 \text{ } \Omega^{-1} \text{ cm}^{-1}$ ) even at the lowest  $T$ , indicating the opening of only a pseudogap in  $\text{BaV}_{13}\text{O}_{18}$ . This is quite different from the formation of a real gap in  $\text{BaV}_{10}\text{O}_{15}$  [5], which exhibits a V trimerization and an insulating ground state below 130 K. The integrated value of  $\sigma(\omega)$  (spectral weight) below 0.2 eV, which approximately corresponds to the isosbestic point of the conductivity spectra, is plotted as a function of  $T$  in Fig. 4(c); the decrease in the spectral weight is correlated with the phase transition at  $T_{co} \sim 200$  K, particularly for  $\sigma_a(\omega)$ . This indicates that the opening of a pseudogap in the  $\sigma(\omega)$  spectra is caused by a phase transition at  $T_{co}$ . The inset in Fig. 4(c) shows the spectral weight as a function of cutoff  $\hbar\omega$  for the 240 and 5 K spectra. The spectral weights for the two temperatures almost merge at  $\sim 0.6$  eV for both  $\sigma_a(\omega)$  and  $\sigma_c(\omega)$ , indicating that the transfer of the spectral weight occurs within this energy scale. It should be pointed out that this energy scale of spectral-weight transfer is comparable to or smaller than that of various transition-metal oxides exhibiting charge ordering at around 200 K [11–14].

As discussed above, the dc resistivity measurement indicates a metallic characteristic of sample 2 below 50 K. In

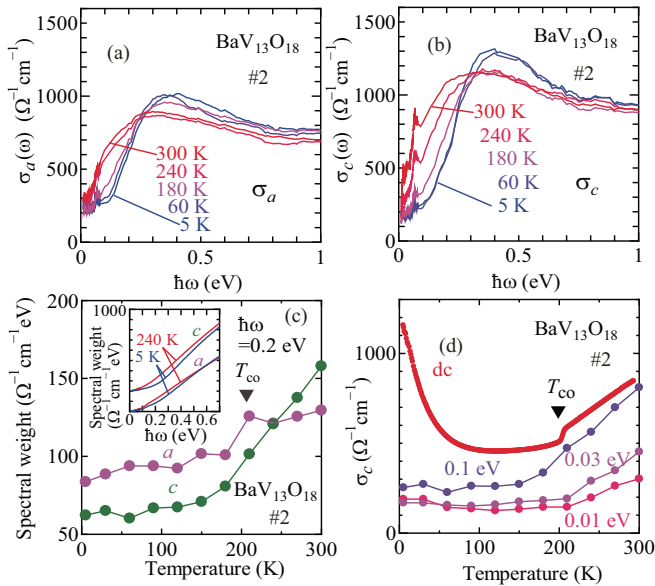


FIG. 4. (Color online) (a, b) Optical conductivity spectra at various temperatures along (a) the  $a$  axis and (b) the  $c$  axis. (c) Integrated value of optical conductivity up to 0.2 eV as a function of temperature. Inset: Spectral weight as a function of cutoff  $\hbar\omega$ , where data are offset for clarity. (d) Value of optical conductivity at various values of  $\hbar\omega$  and dc conductivity as a function of temperature.

Fig. 4(d), the values of optical conductivity at various values of  $\hbar\omega$  and dc conductivity are plotted as a function of  $T$ . The increase in conductivity below 50 K observed for the dc values, indicative of Kondo-singlet formation below  $T_K$ , is not observed in the optical conductivity down to  $\hbar\omega = 0.01$  eV. This indicates that the Drude component responsible for metallic conduction below 50 K exists only below 0.01 eV [8]. Assuming that the number of carriers is 1/13, the total number of V ions, and that the effective mass of the carriers is 50

times the free electron mass as derived from the specific heat measurement, the estimated Drude weight [integrated value of  $\sigma(\omega)$ ] is  $20 \Omega^{-1} \text{ cm}^{-1} \text{ eV}$ . This is nearly consistent with the possible Drude weight for the  $\sigma_c(\omega)$  spectrum at 10 K below 0.01 eV, which reaches  $1200 \Omega^{-1} \text{ cm}^{-1}$  at 0 eV. Note that in various heavy-fermion compounds, a small Drude spectrum appears below  $T_K$  in the  $\hbar\omega$  range far below 0.01 eV [15–20].

It should be pointed out that a spontaneous separation of spin-singlet clusters and magnetic moments in the crystal has been observed in several transition-metal oxides, for example, spinel  $\text{AlV}_2\text{O}_4$ , where spin-singlet V heptamers and lone magnetic  $\text{V}^{3+}$  ions are formed [21], and  $\text{Ba}_2\text{V}_{13}\text{O}_{22}$ , where spin-singlet V trimers and lone magnetic  $\text{V}^{4+}$  ions are formed [6]. However, the ground state of such compounds is insulating, meaning that the magnetic moments remain localized down to the lowest  $T$ . In this sense,  $\text{BaV}_{13}\text{O}_{18}$  with oxygen offstoichiometry belongs to a new class of materials in which the magnetic moments that are separated from the spin-singlet clusters (V tetramers) at high temperatures are coupled with itinerant carriers again and form heavy-mass quasiparticles at low temperatures.

In summary, two single crystals of  $\text{BaV}_{13}\text{O}_{18}$  were studied, one of which is close to stoichiometric and exhibits two phase transitions, at  $T_{\text{co}} \sim 200$  K and  $T_{\text{tr}} = 65$  K, and the other of which is rather off-stoichiometric and exhibits only the high- $T$  phase transition at  $T_{\text{co}}$ . It was found that the ground state of the crystal exhibiting the low- $T$  phase transition ( $T_{\text{tr}}$ ) is insulating, while the crystal in which  $T_{\text{tr}}$  is absent exhibits a metallic ground state. For the latter crystal, the localized magnetic moments that appear below  $T_{\text{co}}$  act as scattering centers for the itinerant carriers above 50 K but are coupled with itinerant carriers and form heavy-mass quasiparticles below 50 K. It was also found that the phase transition at  $T_{\text{co}}$  induces a pseudogap in the optical conductivity spectrum for  $\text{BaV}_{13}\text{O}_{18}$ .

We appreciate the help of T. Konishi with the specific-heat measurement. This work was supported by a Grant-in-Aid for Scientific Research B (No. 25287090) from JSPS.

- [1] M. Ikeda, Y. Nagamine, S. Mori, J. E. Kim, K. Kato, M. Takata, and T. Katsufuji, *Phys. Rev. B* **82**, 104415 (2010).
- [2] M. Ikeda, T. Okuda, K. Kato, M. Takata, and T. Katsufuji, *Phys. Rev. B* **83**, 134417 (2011).
- [3] K. Iwasaki, H. Takizawa, K. Uheda, T. Endo, and M. Shimada, *J. Solid State Chem.* **158**, 61 (2001).
- [4] K. Iwasaki, H. Takizawa, H. Yamane, S. Kubota, J. Takahashi, K. Uheda, and T. Endo, *Mater. Res. Bull.* **38**, 141 (2003).
- [5] T. Kajita, T. Kanzaki, T. Suzuki, J. E. Kim, K. Kato, M. Takata, and T. Katsufuji, *Phys. Rev. B* **81**, 060405 (2010).
- [6] J. Miyazaki, K. Matsudaira, Y. Shimizu, M. Itoh, Y. Nagamine, S. Mori, J. E. Kim, K. Kato, M. Takata, and T. Katsufuji, *Phys. Rev. Lett.* **104**, 207201 (2010).
- [7] K. Takubo, T. Kanzaki, Y. Yamasaki, H. Nakao, Y. Murakami, T. Oguchi, and T. Katsufuji, *Phys. Rev. B* **86**, 085141 (2012).
- [8] See Supplemental Material at <http://link.aps.org/supplemental/10.1103/PhysRevB.89.140401> for details on single-crystal growth and characterization, analysis of the  $T$  dependence of resistivity, optical reflectivity normal to the sample surface that is not parallel to symmetric planes in the crystal, and optical spectra in the far-infrared region.
- [9] M. Hoshino, T. Kajita, T. Kanzaki, M. Uchida, Y. Tokura, and T. Katsufuji, *Phys. Rev. B* **85**, 085106 (2012).
- [10] C. A. Bridges, J. E. Greedan, and H. Kleinke, *J. Solid State Chem.* **177**, 4516 (2002).
- [11] H. L. Liu, S. L. Cooper, and S.-W. Cheong, *Phys. Rev. Lett.* **81**, 4684 (1998).
- [12] T. Ishikawa, K. Ookura, and Y. Tokura, *Phys. Rev. B* **59**, 8367 (1999).
- [13] T. Ishikawa, S. K. Park, T. Katsufuji, T. Arima, and Y. Tokura, *Phys. Rev. B* **58**, R13326 (1998).
- [14] T. Katsufuji, T. Tanabe, T. Ishikawa, Y. Fukuda, T. Arima, and Y. Tokura, *Phys. Rev. B* **54**, R14230 (1996).

- [15] M. Scheffler, M. Dressel, M. Jourdan, and H. Adrian, *Nature* **438**, 1135 (2005).
- [16] B. C. Webb, A. J. Sievers, and T. Mihalisin, *Phys. Rev. Lett.* **57**, 1951 (1986).
- [17] L. Degiorgi, *Rev. Mod. Phys.* **71**, 687 (1999).
- [18] D. A. Bonn, J. D. Garrett, and T. Timusk, *Phys. Rev. Lett.* **61**, 1305 (1988).
- [19] E. J. Singley, D. N. Basov, E. D. Bauer, and M. B. Maple, *Phys. Rev. B* **65**, 161101 (2002).
- [20] A. A. Brown Holden, G. M. Wardlaw, M. Reedyk, and J. L. Smith, *Phys. Rev. Lett.* **91**, 136401 (2003).
- [21] Y. Horibe, M. Shingu, K. Kurushima, H. Ishibashi, N. Ikeda, K. Kato, Y. Motome, N. Furukawa, S. Mori, and T. Katsufuji, *Phys. Rev. Lett.* **96**, 086406 (2006).